

Mesoscale circulation in the Alaskan Stream area

S.V. Prants, A.G. Andreev, M.Yu. Uleysky, M.V. Budyansky

*Pacific Oceanological Institute of the Russian Academy of Sciences,
43 Baltiiskaya st., 690041 Vladivostok, Russia*

Abstract

The Alaskan Stream is the northern boundary current in the subarctic North Pacific. This area is characterized by significant temperature, salinity and density differences between coastal and open-ocean waters and strong mesoscale dynamics. In this paper we demonstrate the transport pathways of Alaskan Stream water in the eastern subarctic Pacific and the eastern Bering Sea from October 1, 1994 to September 12, 2016 with the help of altimetry-based Lagrangian maps. A mesoscale eddy activity along the shelf-deep basin boundaries in the Alaskan Stream region and the eastern Bering Sea is shown to be related with the wind stress curl in the northern North Pacific in winter. A significant correlation is found between the concentration of chlorophyll *a* in the Alaskan Stream area and eastern Bering Sea in August – September and the wind stress curl in the northern North Pacific in November – March. The mesoscale dynamics, forced by the wind stress curl in winter, may determine not only lower-trophic-level organism biomass but also salmon abundance/catch in the study area.

Keywords: Alaskan Stream, eastern Bering Sea, transport pathways, Lagrangian maps, mesoscale eddies, salmon catch

1. Introduction

The Alaskan Stream (AS) is the northern boundary current of the North Pacific Subarctic Gyre flowing westward along the shelf-break to the south of the Alaska Peninsula and the Aleutian archipelago. The AS is a narrow (<100 km), deep (>5000 m) and high-speed current with the transport of the order of $14\text{--}40 \cdot 10^6 \text{ m}^3 \text{ s}^{-1}$ (Favorite, 1974; Ueno et al., 2010). Portions of the AS flow through the Aleutian passes form the Aleutian North Slope Current (Fig. 1), the narrow and high speed current that flows northeastward along the north slope of the Aleutian Islands (Stabeno et al., 2009), and the Bering Slope Current flowing north-westward along the eastern shelf-break of the Bering Sea (BS) (Favorite, 1974; Stabeno and Reed, 1994; Johnson et al., 2004). The northward flow of the AS water through the Aleutian passes is a main source of nutrients and heat for the BS ecosystem (Stabeno et al., 2005). The variations in the Alaska Gyre waters supply, caused by the AS, lead to interannual variations in the dissolved oxygen and temperature in the intermediate layer of the Okhotsk Sea and western subarctic Pacific area (Andreev and Baturina, 2006). Enhancement of the AS flow is accompanied by an increase in sea surface temperature and decreasing ice area in the Okhotsk Sea in winter and can be considered as direct and indirect causes of a reduction in the chlorophyll *a* concentration and large-sized zooplankton biomass in the eastern Okhotsk Sea in winter-spring (Prants et al., 2015).

Mesoscale variability is an important factor in the eastern subarctic Pacific and BS dynamics (e.g., Okkonen et al., 2001, 2003, 2004; Ladd et al., 2007). Mesoscale eddies enhance the cross-shelf exchange of macronutrients, iron and phytoplankton and zooplankton populations (e.g., Johnson et al., 2005; Okkonen

Email address: prants@poi.dvo.ru (S.V. Prants)

URL: <http://dynamlab.poi.dvo.ru> (S.V. Prants)

et al., 2003). Crawford et al. (2005, 2007); Ueno et al. (2010); Brown and Fiechter (2012) have indicated that such eddies play a significant role in controlling time and space patterns of chlorophyll *a* and may, therefore, determine the biological productivity and ecological function in the region. Interannual and decadal modulations of the eastern subarctic Pacific open-ocean ecosystems may be explained by analyzing statistics of eddy-induced cross-shelf transport (Combes et al., 2009). The impact of mesoscale eddies on the circulation and biology in the eastern BS have been examined by many authors (e.g., Okkonen et al., 2004; Mizobata et al., 2002, 2006; Ladd et al., 2012). Instabilities in the Bering Slope Current, wind forcing, topographic interactions and flow through the eastern Aleutian passes have been suggested to be possible eddy-generation mechanisms. Analysis of the SSH time-series in 2002–2012 at the eastern boundary of the subarctic gyre demonstrated that the year-to-year changes of the SSH in the anticyclonic eddies were related to the wind stress curl in winter. It was assumed that spin up of the subarctic cyclonic gyre, forced by the wind stress curl, may enhance the anticyclonic eddy activity in the AS area (Prants et al., 2013a).

In this study we focus at the AS transport pathways by using altimetry-based Lagrangian maps and forcing patterns that contribute to the interannual variability of the mesoscale dynamics and the chlorophyll *a* concentration in the east BS and AS area. We show that the intensity of AS anticyclonic eddies and anticyclonic eddies in the south-eastern BS is determined by the wind stress curl (WSC) in the northern North Pacific in November–March. There is a significant correlation between the concentration of chlorophyll *a* at the deep basin margins in the BS and eastern subarctic Pacific in August–September and the WSC in the northern North Pacific in winter. Our results indicate that mesoscale dynamics in the eastern BS and AS areas may determine not only lower-trophic-level organism (the autotrophic phytoplankton) biomass but also the salmon abundance/catch.

The paper is organized as follows. Section 2 describes briefly the data we use and the Lagrangian methods we apply to study transport pathways, origin, history and fate of different water masses. The next section 3 with the main results consists of two parts. Firstly, we study a correlation between the WSC in the northern North Pacific in winter and mesoscale eddy activity along the deep basin boundaries in the AS region and the eastern BS. The altimetry-based Lagrangian simulation is used to track the penetration of AS and open-ocean waters into the eastern BS. Secondly, we study impacts of the mesoscale activity on chlorophyll *a* concentration in the area and its correlation with salmon abundance and catch. Section 4 discusses possible physical mechanisms of the correlations found.

2. Data and methods

Geostrophic velocities and sea surface heights (SSHs) were obtained from the AVISO database (<http://www.aviso.altimetry.fr>) archived daily on a $1/4^\circ \times 1/4^\circ$ grid from October 1, 1994 to September 12, 2016. The distributed global product combines altimetric data from the TOPEX/POSEIDON mission, from Jason-1 for data after December 2001 and from Envisat for data after March 2002. The meridional and zonal velocities and SSHs are gridded on a $1/4^\circ \times 1/4^\circ$ Mercator grid, with one data file every day.

To compute the WSC ($\text{curl}_z(\partial\tau_y/\partial x - \partial\tau_x/\partial y)$, where τ_y and τ_x are respectively meridional and zonal wind stress components in the northern North Pacific) we used the monthly wind stress dataset from the NCEP reanalysis. Ocean chlorophyll *a* concentration data have been obtained from monthly composites from MODIS satellite imagery of ocean color (Level-3 product) with a horizontal resolution of 9 km on a regular grid (<http://oceancolor.gsfc.nasa.gov>). The salmon catch statistic was downloaded from the North Pacific Anadromous Fish Commission website (<http://www.npafc.org>). ARGO floats data (tracks, seawater temperature and salinity) and bottle oceanographic data (temperature, salinity, nutrients and chlorophyll *a* concentration) have been provided by the National Oceanographic Data Center (<http://www.nodc.noaa.gov>).

Lagrangian maps are geographic plots of Lagrangian indicators versus simulated particle’s initial positions. We used before as Lagrangian indicators different functions of particle’s trajectory (Prants et al., 2013b, 2017). They have been shown in recent years to be useful for studying large-scale transport and mixing in the ocean including propagation of radionuclides in the western North Pacific after the accident at the Fukushima Nuclear Power Plant (Budyansky et al., 2015) and finding of potential fishing grounds (Prants et al., 2014). In order to track penetration of the AS and open-ocean waters into the eastern BS,

we use in this paper a special kind of the Lagrangian maps which we call the origin maps. Being computed backward in time, the origin maps show where the waters came from to a study area and from which water masses a studied eddy consists of. They are computed as follows.

The vast area in the northern North Pacific, $50.0^\circ\text{N} - 65.0^\circ\text{N}$, $160.0^\circ\text{E} - 145.0^\circ\text{W}$, is seeded each three days with a large number of virtual particles for the period of time from October 1, 1994 to September 12, 2016. Their trajectories in the altimetric AVISO velocity field are computed backward in time for a year solving advection equations for passive particles with a fourth-order Runge–Kutta scheme

$$\frac{d\lambda}{dt} = u(\lambda, \varphi, t), \quad \frac{d\varphi}{dt} = v(\lambda, \varphi, t), \quad (1)$$

where u and v are angular zonal and meridional altimetric geostrophic velocities, φ and λ are latitude and longitude, respectively. Bicubical spatial interpolation and third order Lagrangian polynomials in time are used to interpolate the velocity field.

We are interested in three water masses and their transport pathways. To track the AS waters, the section along the meridian $x_0 = 145^\circ\text{W}$ from $y_0 = 58^\circ\text{N}$ to $y_0 = 60^\circ\text{N}$ is fixed. The particles, which crossed that section in the past, are colored in red on the origin Lagrangian maps. The open-ocean particles, which crossed the section $x_0 = 160.0^\circ\text{E} - 164.0^\circ\text{W}$, $y_0 = 50.0^\circ\text{N}$ in the past, are colored in green. The eastern BS particles, which crossed the section from 177.0°E , 62.0°N to 164°W , 55.0°N in the past, are colored in blue (see the yellow line Fig. 2a). We removed from consideration all the particles entered into any AVISO grid cell with two or more corners touching the land in order to avoid artifacts due to the inaccuracy of the altimetry-based velocity field near the coast. Due to impact of the coast, the Alaskan Coastal Current pathways in the Pacific Ocean and BS (see, e.g., Schumacher et al., 1989; Stabeno et al., 2005) have not been analyzed using altimetry-based Lagrangian maps. The corresponding colored Lagrangian maps demonstrate clearly transport pathways of those water masses in the study area.

It is useful to identify locations in the ocean with zero geostrophic velocity. In the theory of dynamical systems, these can be termed “elliptic and hyperbolic stagnation points” that are indicated on the Lagrangian maps by triangles and crosses, respectively. The elliptic points, located mainly in the centers of eddies, are those points around which the motion of water is stable and circular. The upward oriented blue triangles mark centers of anticyclones and downward oriented triangles in red indicate cyclones. The hyperbolic points, located mainly between and around eddies, are unstable stagnation points with the direction along which water parcels converge to such a point and another direction along which they diverge. The existence of hyperbolic areas in the ocean have been recently confirmed by tracks of drifters in the western North Pacific (Prants et al., 2016).

3. Results

3.1. The Alaskan Stream eddies and transport pathways of the Alaskan Stream and open-ocean Pacific waters into the eastern Bering Sea revealed by the Lagrangian maps

The strong and narrow AS in the northern Pacific, the Aleutian North Slope Current and the Bering Slope Current in the BS are clearly visible in the altimetric AVISO velocity field averaged for February (Fig. 1a) from 1994 to 2016. The main inflow of the AS waters into the BS occurs through the Amchitka (180°W) and Amukta (172°W) Passes. In August, the surface circulation in the eastern BS is determined by mesoscale anticyclonic and cyclonic activity. The mesoscale anticyclones in the area of the Bering Slope Current are topographically constrained with the Navarin, Zhemchug and Pribilof canyons (Fig. 1b). An intensification of the southwestward flow of AS water in the northern North Pacific and the north-northwestward flow of AS water in the BS are typically observed in November–March when the Aleutian Low pressure cell is activated. Off-shore AS meanders are related to the mesoscale anticyclonic and cyclonic eddies. The origin Lagrangian maps in Figs. 2a–c and 3a–d and the surface salinity and nitrate distributions in Figs. 3e and f show that less saline and relatively low nitrate AS waters (marked by the red color) intrude into the BS through the Aleutian passes and then flow northwestward along the Bering slope. The small and large eddies in the Aleutian Islands area stimulate inflow of the AS water and the open-ocean subarctic water (marked by green) into the BS.

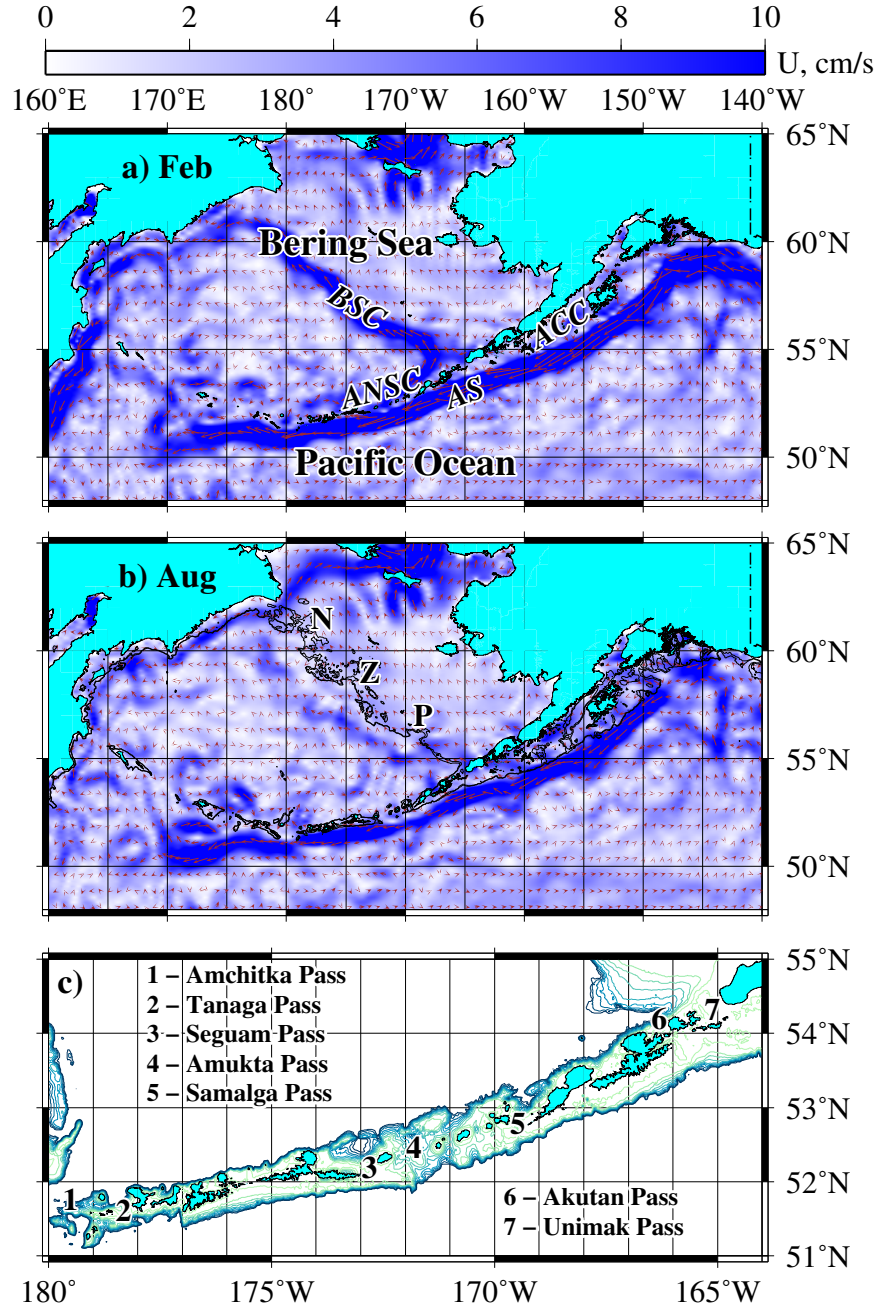


Figure 1: The altimetric AVISO velocity field averaged for a) February and b) August from 1994 to 2016. c) The Aleutian passes. Abbreviations: ACC — Alaska Coastal Current, ANSC — Aleutian North Slope Current, AS — Alaskan Stream, BSC — Bering Slope Current, N — Navarin Canyon, Z — Zhemchug Canyon and P — Pribilof Canyon.

The southwestward drift of the AS mesoscale anticyclones along the Alaskan Peninsula and eastern Aleutian Islands forced the AS water southward into the deep Pacific basin and enhanced the AS and open-ocean water to inflow in the BS (Figs. 1a and b, Fig. 3a–d). We focused on the mesoscale anticyclonic eddies originating in the northern part of the Gulf of Alaska and advected by the AS along the Pacific Ocean side of the eastern Aleutian Islands. These eddies have typically an elliptical shape with a dimension of about 150×200 km with the centers (the elliptic points) located over the axis of the Aleutian bottom trench. Inspecting the daily Lagrangian maps, we have found that one of such eddies, which we call ASAC 2003–2004, originated in the northern part of the Gulf of Alaska in winter 2002. In summer and fall 2002, it was relatively weak and located to the southwest off the Kodiak Island with the center at around 55.5° N, 153° W. The reinforcement and enlargement of this eddy occurred in January–March 2003 southward of the Alaskan Peninsula in the area 53° N– 55° N, 156° W– 158° W when the WSC over the northern North Pacific increased significantly.

The ASAC 2003–2004 is clearly seen on the origin Lagrangian map in Fig. 2a with the center at around 54.2° N, 157° W on February 15, 2003. It consists of the core with a “white” water, a periphery with the AS “red” water surrounded by the “green” open-ocean waters. The intensification of this eddy was accompanied by advection of the open-ocean water by a cyclonic eddy toward the western and southern edges of the ASAC 2003–2004 (Figs. 2a and c) and thereby an increase of the temperature, salinity and density differences between the ASAC 2003–2004 and outside open-ocean waters (Figs. 2d–f). The ARGO CTD data (buoys nos. 49070 and 4900176) demonstrate that the ASAC 2003–2004 had a warmer, less-saline and less-dense core than the open-ocean subarctic water. During its southwestward drift in 2004, the ASAC 2003–2004 controlled supply of the AS water (Fig. 2b) and open-ocean subarctic water into the BS through the Aleutian passes (Fig. 3b).

The eddy, which we call ASAC 2005–2006, was not advected to the 53° N– 55° N, 156° W– 158° W area in winter 2004 during the period of low WSC in the northern North Pacific but stayed southward of Kodiak Island and was relatively weak (Ladd et al., 2007). We observed its activation and reinforcement in winter 2005 when the WSC over the northern North Pacific increased. During 2005 and 2006, the ASAC 2005–2006 forced the transport of AS and open-ocean waters into the BS (see Figs. A.8a and b). Figures A.9a and b in Appendix show the vertical distributions of temperature, salinity and potential density in the ASAC 2005–2006 and outside waters in September 2005 and September 2006. Similar to the ASAC 2003–2004 (Figs. 2d–f), the ASAC 2005–2006 core was composed of relatively low salinity (33.7–33.9) and low density (26.7–26.9) waters. The temperature of waters inside of the anticyclone was 1–2 $^\circ$ C higher than outside it.

An increase of the WSC in winter 2008 led to enlargement and strengthening of the eddy ASAC 2008–2009 in the 53.5° N– 55° N, 156° W– 158° W region and formation of a second anticyclonic eddy. During its southwestward drift in 2008 and 2009, the anticyclonic eddies centered at 51.5° N, 170° W and 52.4° N, 167° W in August 16, 2009 forced the intrusions of AS water (summer 2008) and open-ocean Pacific water (summer 2009) into the BS (Figs. 3c and d). In winter 2010, the eastern anticyclonic eddy was advected to the south of the Aleutian Islands and the western eddy drifted along the Aleutian Islands to the western subarctic Pacific. In fall 2010 and winter 2011, the ASAC 2008–2009 was observed in the central part of the Western Subarctic Gyre with the elliptic point at 51° N, 170° E.

The supply of the AS water through the Aleutian passes leads to formation and strengthening of anticyclonic eddies in the eastern BS. In January–February 2003, an inflow of the AS water through the Amchitka Pass led to formation of the anticyclonic eddy (the red patch centered at around 52.5° N, 179° W) in the southern BS (Fig. 2a). The generation of the “Pribilof mesoscale anticyclonic eddy 2004” in the BS was observed in the eastern Aleutian Passes in spring 2004. In May 2004 it intensified probably due to a density difference at its edges between the “red” AS water and “green” open-ocean water. In June 2004 its center was at the point 54.5° N, 168° W (see Fig. A.8c). In July–September it occupied its position to the southwest of Pribilof canyon with the elliptic points at 55.5° N, 171° W (Fig. 3b). In October 2004 it moved westward to the deep BS. During its stay in the Bering Slope Current region, the Pribilof mesoscale anticyclonic eddy 2004 trapped the “blue” BS shelf water and wound around it (Fig. 3b). The penetration of the BS outer shelf water into the eddy at that place has been shown by the CTD observations conducted in June 1997 (Ladd et al., 2012) (see Fig. A.8d).

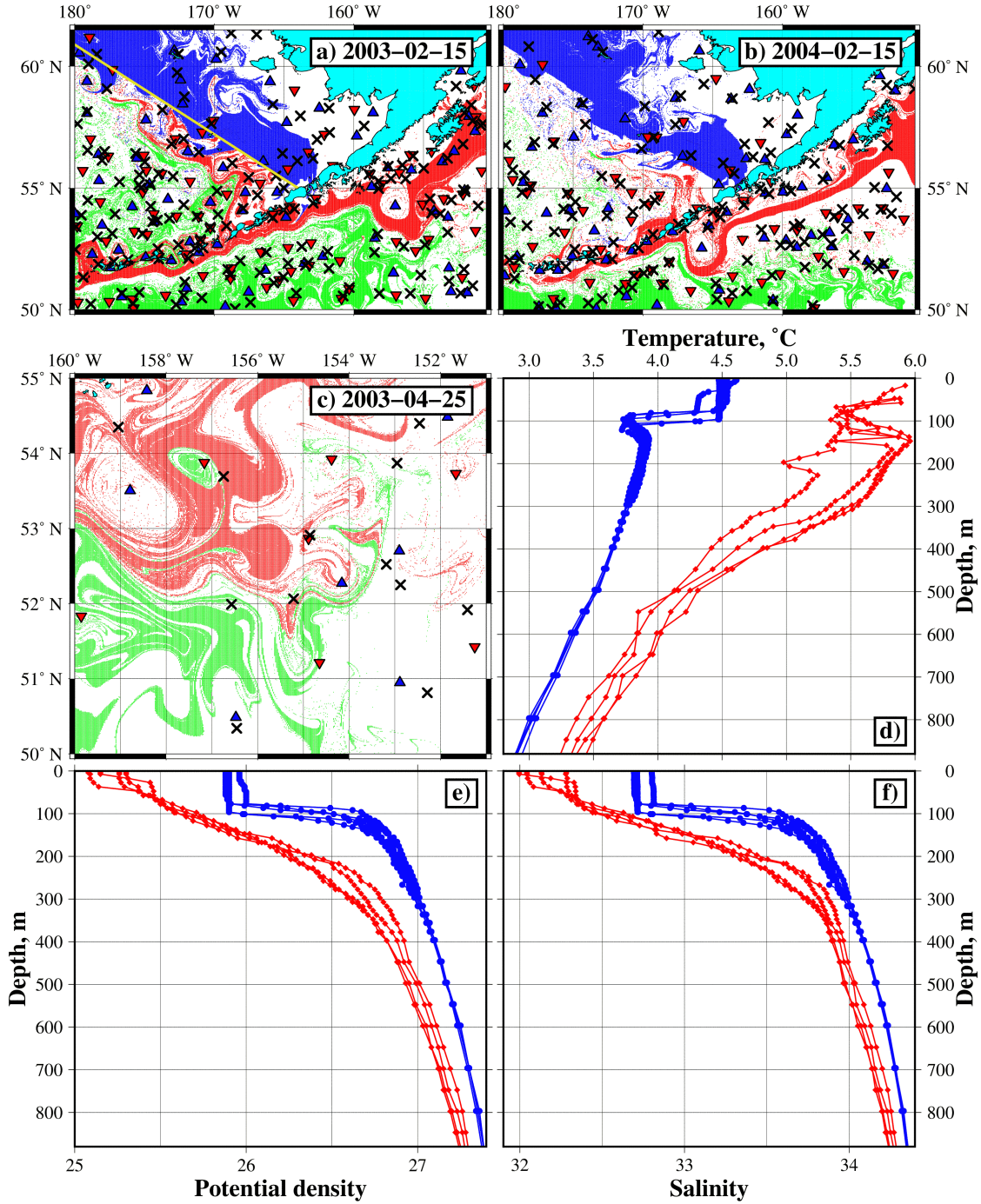


Figure 2: a) and b) The origin Lagrangian maps show the intrusion of AS waters (red) and off-shore subarctic waters (green) from the northern Pacific into the eastern BS through the Aleutian passes in February 2003 and February 2004. The penetration of the BS shelf waters into the deep basin of the eastern BS is demonstrated by the blue color. c) The map on April 24, 2003 with the AS anticyclone ASAC 2003–2004 centered at 53.5° N, 158.8° W and the eastern subarctic cyclone (the green patch of open-ocean water centered 51.2° N, 154.6° W). d)–f) The vertical distributions of temperature, salinity and relative density in the ASAC 2003–2004 (the red profiles) and the subarctic cyclone with open-ocean water (the blue profiles) in March–May 2003 (data from the ARGO buoys nos. 49070 and 4900176). Elliptic (stable) stagnation points with zero mean velocity at the fixed date are indicated by the downward and upward oriented triangles which mark cyclones and anticyclones, respectively.

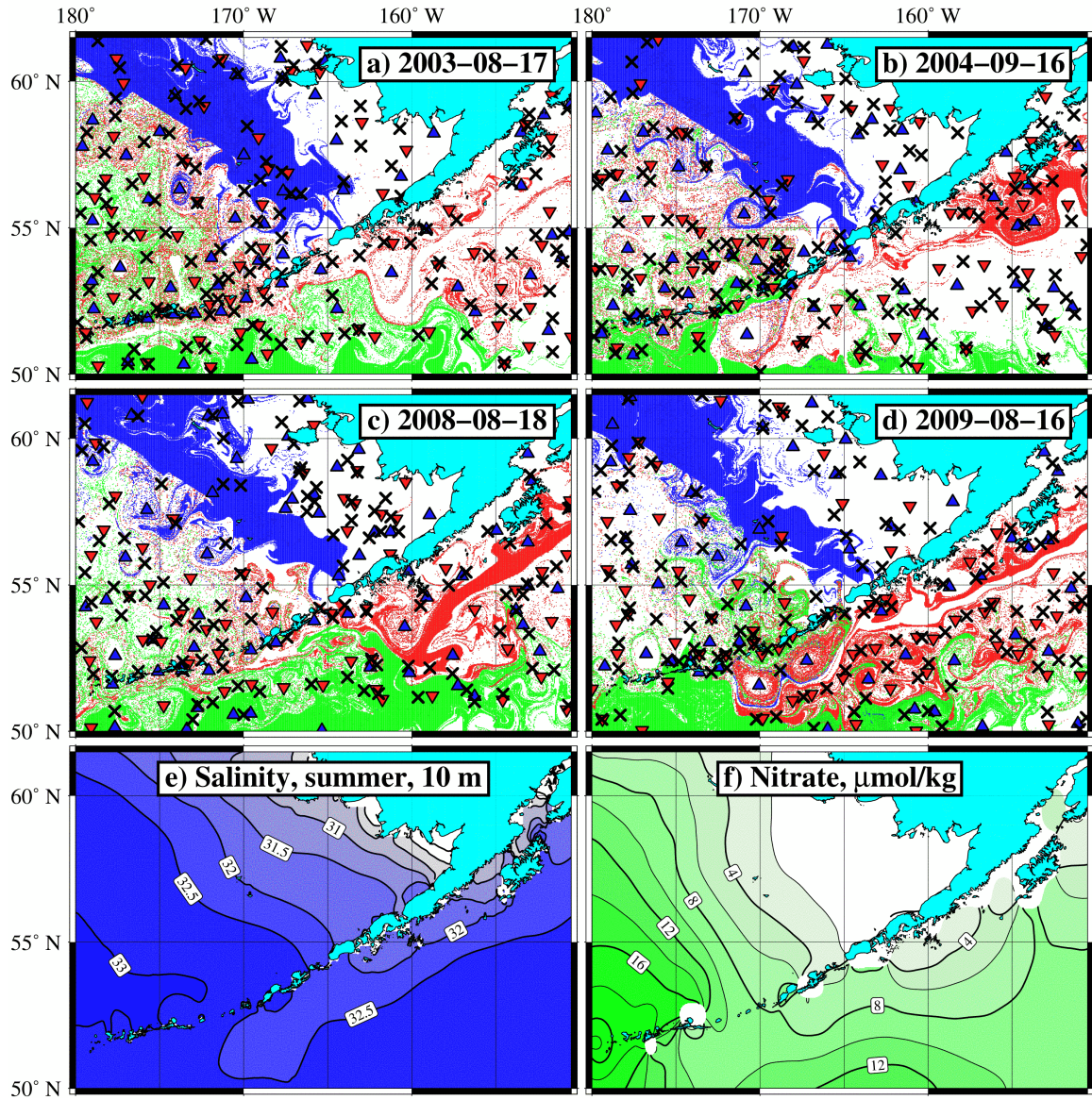


Figure 3: a)–d) The origin Lagrangian maps demonstrate the impact of the AS anticyclonic eddies on the supply of “red” AS waters and “green” open-ocean subarctic waters from the northern Pacific into the eastern BS and penetration of the “blue” BS shelf waters into the deep BS basin in August and September 2003, 2004, 2008 and 2009. e) and f) The distributions of the salinity and nitrate concentrations in the surface waters (10 m) of the northern Alaska and eastern BS in summer (July–September, World Ocean Atlas 2013, 1° grid).

3.2. A correlation between the mesoscale eddy activity in the Alaskan Stream region and the eastern Bering Sea and the wind stress curl in the northern North Pacific in winter

The strength and position of the Aleutian Low pressure cell are the main factors which determine the circulation in the northern North Pacific. The strong Aleutian Low and positive WSC pattern over the northern North Pacific in November–March spin-up the subarctic cyclonic gyre (e.g., [Ishi, 2005](#)). One may assume that that spin-up results in more eddy activity at its northern boundary (the AS region). The anticyclonic eddies contain a core of low-density water that produces an upward doming of the sea surface detectable by satellite altimeters.

The increased (decreased) SSH in AS anticyclonic eddies are associated with the increased (decreased) WSC in the northern North Pacific (46°N – 48°N , 165°E – 170°W) in winter with the correlation coefficient $r = 0.60$ – 0.90 , 2002–2016 (Fig. 4). Amplitude of the steric height variability in the study area is about 2.4 cm (the thermosteric height signal is about 2 cm and halosteric height signal is about 0.4 cm) ([Qiu, 2002](#)), which is several times less than the amplitude of the interannual variations of SSH in the AS area in February and August (around 20 cm) (Figs. 5a and b).

To find a correlation between the WSC and SSH and the velocities at the boundaries of AS anticyclonic eddies, we used monthly averaged SSH and velocities. If the correlation was found to be significant for a two month period (May and June, July and August, etc.) we used the SSH and velocities averaged for May–June, July–August, etc. (see the corresponding figure captions or legends). There is a good correlation with $r = 0.70$ – 0.80 between the monthly averaged SSH along the northern and northeastern boundaries of the Gulf of Alaska and monthly averaged zonal wind stress (55°N – 60°N , 140°W – 150°W) in November–March when the Aleutian Low developed in the northern North Pacific ([Qiu, 2002](#)). The formation of anticyclonic eddies along the northern boundary of the Gulf of Alaska can be related to the along-shore wind and downwelling (see, e.g., [Combes and Di Lorenzo, 2007](#)). However, our results show that reinforcement of the AS anticyclonic eddies southward of the Alaskan Peninsula (53°N – 55°N , 156°W – 158°W) occurs during the periods of increased WSC in the northern North Pacific. The correlation between the SSH in the AS anticyclonic eddies and the WSC is significant for two years (Fig. 4).

Our results demonstrate that the meridional and zonal velocities at the AS eddy boundaries during two years (while the eddies drift southwestward along the western Alaska Peninsula and eastern Aleutian Islands) are determined by the WSC in winter (Figs. 5c and d). The increased WSC in the northern North Pacific enhances the northward flow of the open-ocean subarctic water to the southern boundary of the AS anticyclonic eddies in January–February (Fig. 5e) and thereby increases the density gradient at the eddy edges.

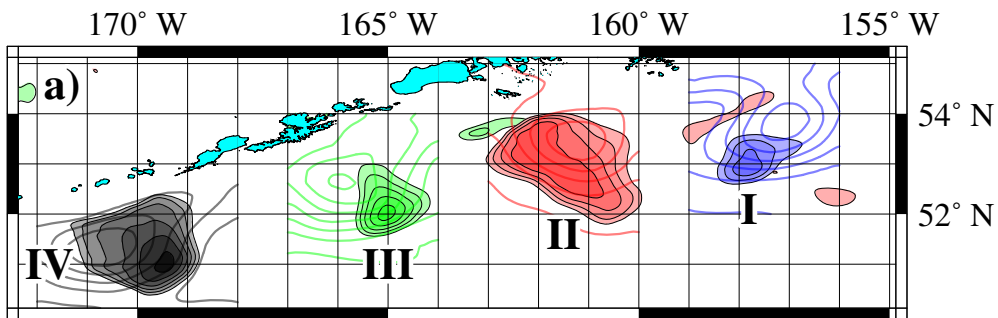


Figure 4: The distribution of the correlation coefficients (0.60–0.90, int. = 0.05) between the change of the WSC (November–March) and SSH in the AS area in March (I), August (II), February (III, 1-yr lagged WSC) and September (IV, 1-yr lagged WSC). The SSH isolines in March and August, 2003 and February and September, 2004.

The changes in the Aleutian Low activity and WSC in the northern North Pacific in winter determine year-to-year changes in velocities in some areas of the eastern BS. An increase (decrease) of the WSC in the North Pacific in November–March is accompanied by increased (decreased) velocities at the boundaries of

the anticyclonic eddies in the central part of the deep BS in summer and fall (Fig. A.10a). An intensification of the Aleutian Low and a large positive WSC result in increasing of the northward flow on the BS outer shelf in the areas located close to the Pribilof, Zhemchug and Navarin canyons (Fig. A.10c). An increase (decrease) of the WSC in the northern North Pacific in November – March with a 1-year lag is accompanied by increased (decreased) velocities at the boundaries of the anticyclonic eddies located in the area of Aleutian North Slope Current in summer and fall (Fig. A.10b).

3.3. Chlorophyll *a* concentration and fish abundance and catch in the area

Mesoscale eddies modulate primary production along the eastern subarctic Pacific shelf break entraining chlorophyll *a*- and iron-rich shelf water while simultaneously transporting nitrate- and silicate-rich basin water to the shelf (see, e.g., Okkonen et al., 2003; Ladd et al., 2005; Crawford et al., 2007). The dominant feature in chlorophyll *a* distribution in the surface layer in the AS region is a contrast between coastal and offshore waters. The coastal waters are productive with high values of chlorophyll *a* concentration ($>3 \mu\text{g/l}$ in August and September), whereas the offshore waters are oligotrophic with low chlorophyll *a* concentration values ($<1 \mu\text{g/l}$).

The chlorophyll *a* pool south of the Alaska Peninsula in summer 2005 and south of the eastern Aleutian Islands in summer 2006 was affected by the mesoscale anticyclonic eddies centered at 53.5°N , 161°W and 52.5°N , 167°W , respectively (Figs. 6a and b). The filaments with high chlorophyll *a* concentration ($1\text{--}2 \mu\text{g/l}$) have been transported off the shelf, wrapping around the mesoscale eddies and then being trapped inside the eddies. The WSC forcing in winter modulates the strength of anticyclonic eddies in the AS area and the velocities at their boundaries. Year-to-year variations in location and strength of those anticyclonic eddies can determine spatio-temporal changes in chlorophyll *a* concentrations in the surface waters in the AS region during August – September. Figures 6c and d show year-to-year changes of the chlorophyll *a* concentration in August – September and the WSC in the northern North Pacific in November – March. Large (in 2003 and 2005) and small (in 2002 and 2004) values of the WSC in the northern North Pacific and, therefore, increased (decreased) velocities at the eddy’s boundaries (Figs. 5c and d) have been accompanied by increased (decreased) chlorophyll *a* concentrations at the boundaries of the AS eddies with no lag (Fig. 6c) and a 1-year lag (Fig. 6d).

Figures A.11a and b show the distribution of chlorophyll *a* concentration in the surface layer in the northern North Pacific and in the BS in August and September 2004 and a difference in the chlorophyll *a* concentration between 2004 and 2003. Large values of the WSC over the northern North Pacific in winter 2003 resulted in strengthening of the AS anticyclonic eddy and change in the velocity field in the eastern BS in 2003 and 2004 while that eddy was drifting along the Aleutian Islands. In August and September 2004, the spots with high values ($1.5\text{--}3 \mu\text{g/l}$) of satellite-measured chlorophyll *a* have been observed in the region of the Aleutian North Slope Current and along the shelf break of the eastern BS (Figs. A.11a and b). In August and September 2004, the surface waters have been significantly enriched by the chlorophyll *a* pigment as compared to August and September 2003. In the central BS, we could see the shelf-break front marking the boundary between low surface chlorophyll *a* and relatively fresh outer shelf water and relatively high surface chlorophyll *a* and more saline basin water. This front is biologically significant because it coincides with the BS “Green Belt”, a region with high primary production that supports an extensive variety of consumer species (see, e.g., Springer et al., 1996; Okkonen et al., 2004)).

Year-to-year changes in the chlorophyll *a* concentrations in the upper surface layer in the eastern BS (similar to the AS region) have been positively correlated ($r = 0.7\text{--}0.8$, 2002–2016) with the WSC in the northern North Pacific in November – March (Fig. 6c). An intensification of the Aleutian Low in winter and thereby an increase of the WSC in the northern North Pacific were accompanied by increased chlorophyll *a* concentration in the surface waters at the BS shelf edge with a 1.5-year lag).

Biomass of autotrophic plankton and concentration of chlorophyll *a* are determined by many factors, such as solar radiation, seawater temperature, macro- and micro-nutrients availability, water column stratification, etc. One of the most important factors, limiting phytoplankton growth in the upper layer in the subarctic North Pacific and the BS in the post-spring-bloom period (July – September), can be a low supply of nutrients with dissolved inorganic nitrogen and silicate considered to be the dominant elements limiting phytoplankton growth. In summer, there is a good agreement between the spatial distributions of salinity and the nitrate

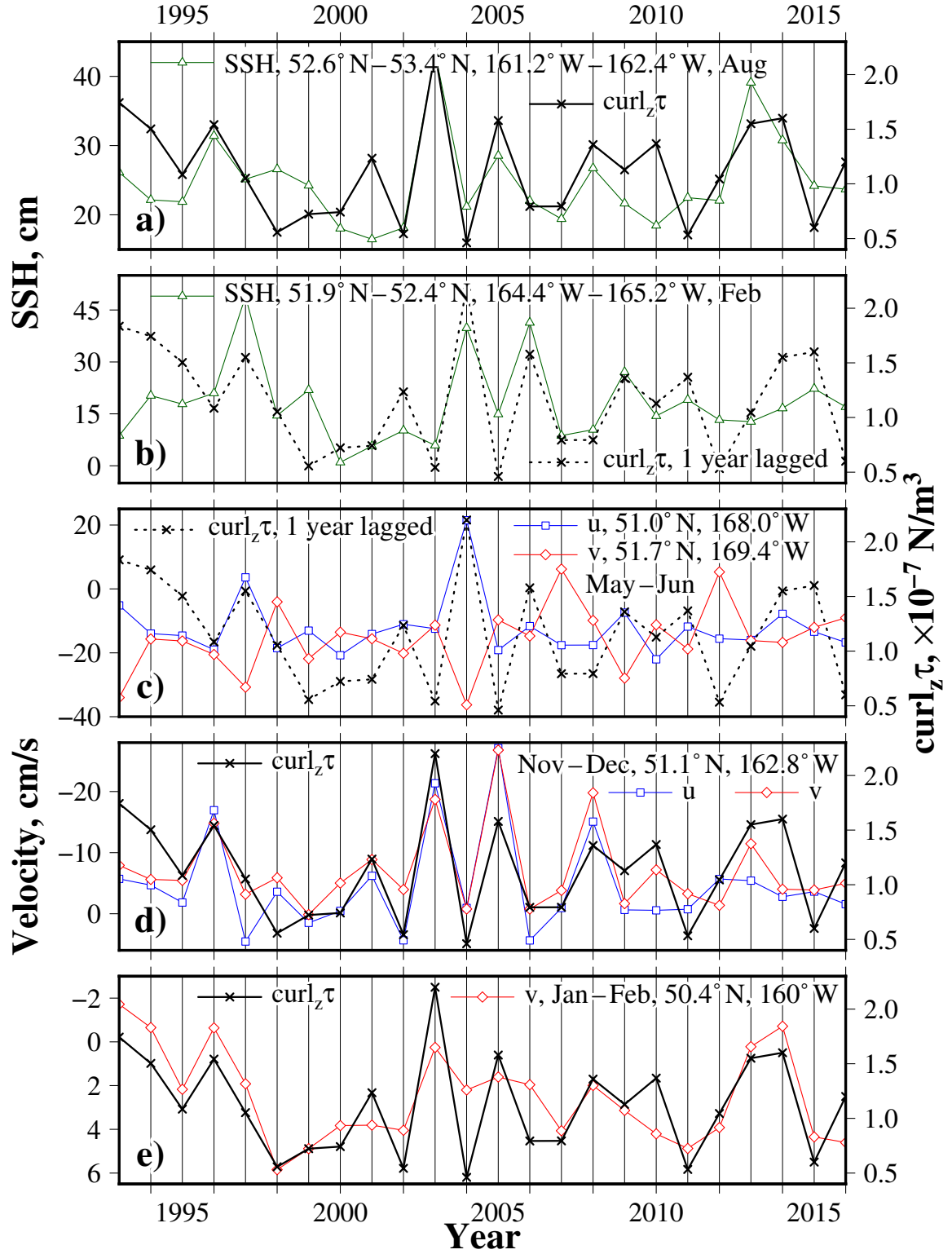


Figure 5: a)–e) The year-to-year changes of the WSC (November–March) in the northern North Pacific, SSH, the meridional and zonal velocities in the AS area.

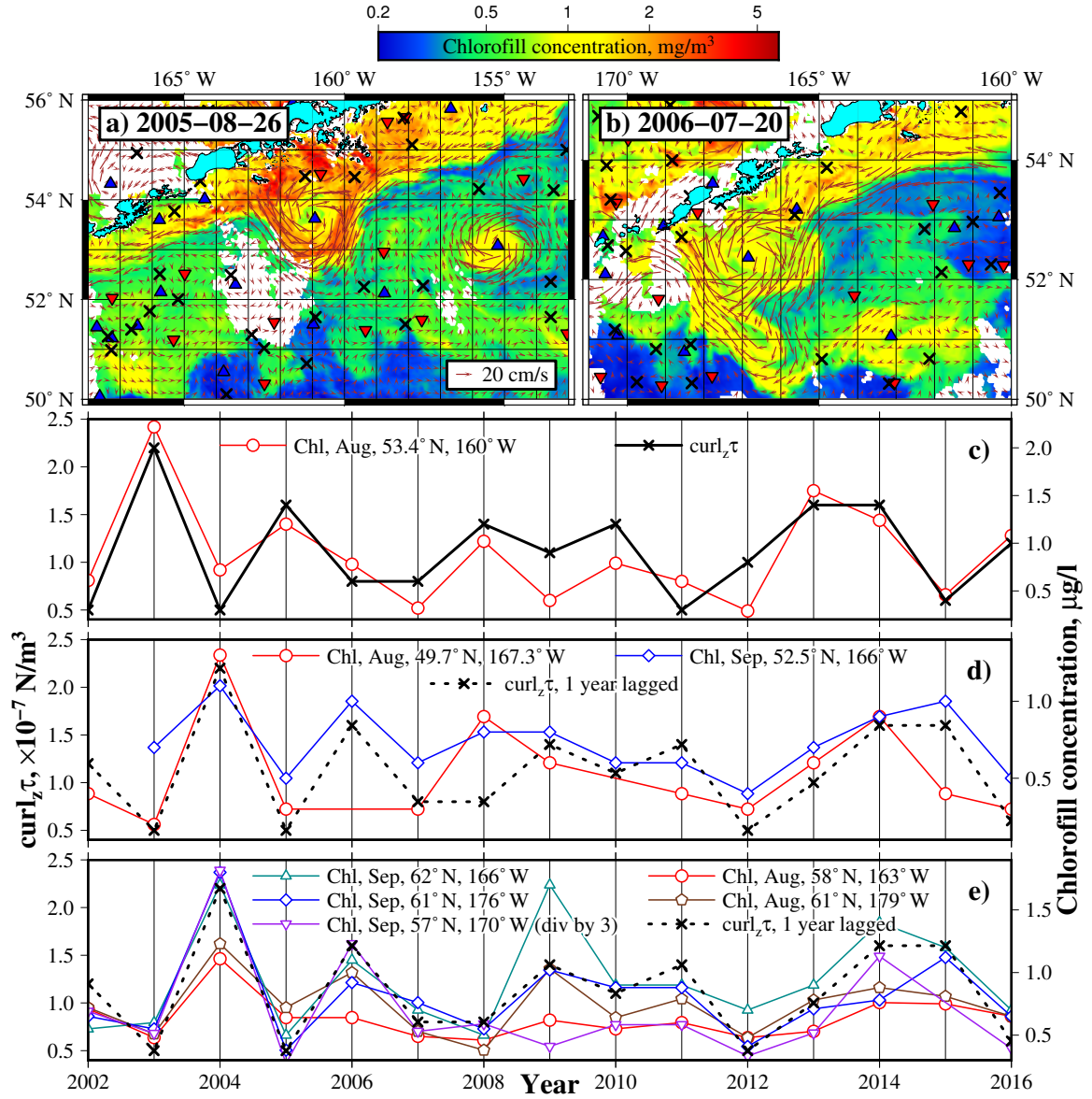


Figure 6: a) and b) Distributions of the chlorophyll *a* concentration (the MODIS data) imposed on the AVISO velocity field on the days indicated. c)–e) Year-to-year changes in the WSC (November–March) in the northern North Pacific and in the chlorophyll *a* concentration in the AS and BS area. Elliptic and hyperbolic (unstable) stagnation points with zero mean velocity are indicated by triangles and crosses, respectively.

concentration in the surface layer in the BS and the eastern subarctic Pacific (Figs. 3e and f). Low salinity (less than 32.2) Alaskan waters are associated with low nitrate concentrations (less than 4–6 $\mu\text{mol kg}^{-1}$) in the upper surface layer. In the subarctic North Pacific and the BS, the vertical distribution of salinity determines a density stratification in the upper layer. Existence of the strong vertical gradient of salinity (a halocline) limits vertical exchange between the surface and deeper layers. Due to tidal mixing in the Aleutian passes (such as the Seguam and Tanaga Passes) (Stabeno et al., 2005), salinity and the concentration of nitrate in the upper surface waters in the BS deep basin reach, respectively, 33 and 15–20 $\mu\text{mol kg}^{-1}$. The nutrients, introduced due to mixing in the passes and then advected northward, are critical to the BS ecosystem.

The vertical profiles of the chlorophyll *a* concentration in the eastern BS in summer are characterized by a subsurface maximum located in the 10–40 m layer (Fig. A.11d). The concentrations of chlorophyll *a* in the upper 40 m layer reach 4–6 $\mu\text{g/l}$. The depth of the chlorophyll *a* maximum location is related to nutrient availability and a water column stratification. The observations, conducted in July 2003 and 2004 in the eastern BS, demonstrate that the shallow (10–20 m) chlorophyll *a* maxima have been related to the waters with strong salinity and density stratifications and with salinities of 32.5–32.8 in the surface layer. For relatively low (32.3) and high surface salinities (33.0), the chlorophyll *a* maxima have been located in the 20–40 m layer. The shallow location of the chlorophyll *a* maximum provides higher chlorophyll *a* concentration in the upper (0–10 m) surface layer captured by the satellite sensors.

Using the relationship between salinity and nitrate concentration (Ladd et al., 2005; Mordy et al., 2005; Stabeno et al., 2005), the difference in satellite-measured chlorophyll *a* concentration in the eastern BS between summer 2003 and summer 2004 (Figs. A.10a and b) can be explained. In summer 2003, the surface salinity was relatively low (32.4) in the most eastern part of the Bering deep basin (54° N–55° N, 170° W–171° W) and relatively high (33.0) in its southern part (53° N–54° N, 172° W–174° W) (Fig. A.10e). In summer 2004, the distribution of salinity in the surface layer in the eastern deep BS was quite uniform with the value of 32.8 (Fig. A.10e).

The salinity distributions in the deep eastern BS in summer 2003 and summer 2004 (Fig. 4Se) are in a good agreement with the water mass distributions demonstrated by the origin Lagrangian maps in Figs. 3a and b. The Lagrangian maps show that in summer 2003 the southeast of the BS was occupied by the “green” open-ocean subarctic (more saline) waters and populated mainly by cyclones, while the BSC area was occupied by the “red” AS (less saline) waters and populated by anticyclonic eddies (Fig. 3a). In summer 2004, the deep eastern BS was composed of spots of open-ocean and AS waters (Fig. 3a) and was characterized by a quite uniform salinity distribution possibly due to the anticyclones eddies activity (Fig. A.11e). The mixing, induced by anticyclonic eddies between the low salinity coastal water and high salinity deep basin water, probably create favourable conditions with nitrate availability and a shallow pycnocline for phytoplankton growth and, thereby, significantly increased the chlorophyll *a* concentration in the upper surface layer in the eastern BS in summer 2004.

The impact of the anticyclonic eddies on the chlorophyll *a* distribution in the AS area can be demonstrated by using a Lagrangian indicator $L = \int_0^T \sqrt{u^2 + v^2} dt$, which is a measure of a distance passed by advected particles. The indicator L is more suitable for detecting and documenting vortex structures than the Lyapunov exponent and displacement of particles D from their initial positions (Prants et al., 2016). A studied area has been seeded at a fixed date with a large number of virtual particles whose trajectories have been computed backward in time for a month in the AVISO velocity field. The L maps visualize not only the very vortex structures but also a history of water masses to be involved in the vortex motion in the past.

In Figures 7a and A.12 we impose distributions of the values of the Lagrangian indicator L in the AS area on the chlorophyll *a* patterns in May 2006, May 2010 and May 2011 with an intermittency of productive coastal waters with high chlorophyll *a* values ($>6 \mu\text{g/l}$) and oligotrophic offshore waters with low chlorophyll *a* values ($<1 \mu\text{g/l}$). The black contours in those figures are isolines of L with the step of 200 geographic minutes. They enclose stable mesoscale eddies, such as ones centered at 52.5° N, 165° W and at 53° N, 164° W. Filaments with high chlorophyll *a* concentration are transported offshore and wrapped around persistent mesoscale eddies existing in the area.

Mesoscale anticyclonic eddies with high primary production in the eastern subarctic Pacific and the eastern BS region are able to influence the zooplankton which could, in turn, support higher trophic levels and create favorable fishing grounds. Distribution, migration paths and growth rate of salmon during its sea period of life are defined by oceanographic conditions at feeding grounds. Mesoscale activity (the scale and strength of eddies, intensity of mesoscale water transport, etc.) is one of the main factors which determines the dimension and spatial structure of salmon feeding grounds (see, e.g., [Sobolevsky et al., 1994](#)). Formation and dynamics of the salmon feeding base are influenced by the mesoscale activity in the region.

Eastern subarctic Pacific and the eastern BS are the main feeding areas for salmon in the northern North Pacific (see, e.g., [Myers et al., 2007](#); [Sato et al., 2009](#)). Figures 7b–d demonstrate year-to-year changes in the WSC in November–March (the 5-years running mean) in the northern North Pacific and annual catch of chum salmon (b, d) and coho salmon (c). The total catch of chum salmon in the western Alaska area was comparatively low from about 1950 to 1970. Catches increased dramatically in 1975–1995 but declined in the late 1990s and slightly increased in 2005–2009 (Figs. 7b and d). The total catches of coho salmon in the central, southwestern and eastern Alaska region and of chum salmon in the western BS were relatively high (30–50 thousands ton and 2–5 thousands ton) from 1980 to mid-1990s but significantly decreased to about 20 thousands ton and 0.5–1 thousands ton in 2000–2010 (Fig. 7c). Strong correlations between the changes in the chum and coho salmon catches in the eastern subarctic Pacific and the BS and the WSC in the northern North Pacific in winter with the coefficient $r = 0.64$ – 0.75 could be related to changes in the mesoscale eddy activity in the study area.

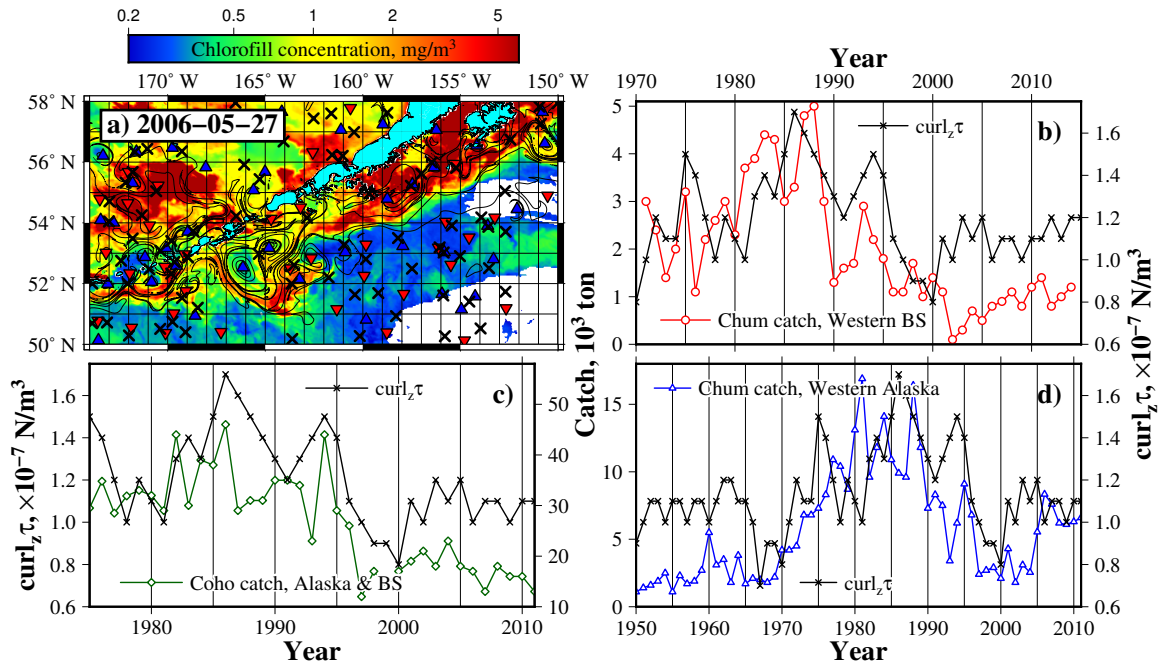


Figure 7: a) The impact of anticyclonic eddies on the chlorophyll *a* distribution (the MODIS data) in the AS area. The black contours are isolines of the Lagrangian indicator L with the step of 200 geographic minutes. Year-to-year changes in the WSC in November–March (the 5-years running mean) in the northern North Pacific and in the annual catch of b) and d) chum salmon and c) coho salmon in the eastern subarctic Pacific and BS.

4. Discussion

The altimetry-based daily computed Lagrangian maps allow tracking of the origin and transport pathways of the AS waters in the northern North Pacific and the BS and facilitate visualization of mesoscale

eddies in the study area. An intensification of the AS flow was observed in November–March when the Aleutian Low developed in the northern North Pacific, and strong positive WSC appeared in the subarctic North Pacific and the BS. In spring–fall, the southward meanders of the AS and the flow of the AS water and open-ocean subarctic water through the Aleutian passes into the BS were caused by mesoscale eddy activity.

Periods of increased eddy activity along margins of the eastern subarctic Pacific may be related to anomalous downwelling wind conditions along the continental margin (see, e.g., [Combes and Di Lorenzo, 2007](#); [Henson and Thomas, 2008](#)). Increased poleward (downwelling favourable) wind stress, increased WSC along the eastern boundary and subsequent increase in the Alaska Current transport and intensification of the cyclonic gyre generate more mesoscale eddies ([Okkonen et al., 2001](#); [Melsom et al., 2003](#); [Ladd et al., 2007](#)). Wind stress curl is expected to be the most important forcing factor for the large-scale variability of circulation in the eastern subarctic Pacific ([Cummins and Mysak, 1988](#)). [Combes et al. \(2009\)](#) concluded that on interannual and longer time scales, the offshore transport of passive particles in the Alaskan Stream does not correlate neither with a large-scale atmospheric forcing, nor with local winds. In contrast, in the Alaska Current region, stronger offshore transport of passive particles coincides with periods of stronger downwelling which triggers development of stronger eddies.

Our results show that strength of the AS anticyclonic eddies (SSH in the eddy’s center and velocities at the boundaries) to the south off the Alaskan Peninsula and the eastern Aleutian Islands are determined by the WSC in the northern North Pacific in November–March. One may assume that that spin-up of the cyclonic gyre in the subarctic Pacific, forced by the WSC in November–March, causes enhanced eddy activity along the continental slope of the Alaskan Peninsula and the Aleutian archipelago. The annual modulation in the cyclonic gyre’s intensity in these areas should be interpreted as a barotropic response to the seasonal WSC forcing. The magnitude of this response is quantifiable by a time-dependent Sverdrup balance ([Bond et al., 1994](#); [Ishi, 2005](#)). Reinforcement and strengthening of the AS eddies occur in the 53°N – 55°N , 156°W – 158°W area. The correlation between the SSH in the eddies, the velocities at their boundaries and the WSC in the northern North Pacific in winter is significant during two years while the eddies have been advected westward. An intensification of the anticyclonic eddies activity is accompanied by an increase of the northward advection of the open-ocean water to the eddy’s boundaries and, thereby, an increase in the density difference between anticyclonic eddies and ambient waters.

The significant correlation between the surface velocities at the outer shelf margin of the eastern BS in summer and fall and the WSC in the North Pacific in winter (Fig. [A.10b](#)) is related probably to the AS and open-ocean water supply to the BS. The increased inflow through the Aleutian passes may enhance eddy variability along the Bering Slope Current by increasing a baroclinic instability ([Mizobata et al., 2008](#)). The supply of low salinity Alaska coastal waters and relatively high salinity open-ocean waters creates zones with significant horizontal salinity and density gradients and, thereby, could enhance the mesoscale dynamics in the eastern BS.

An increase of the WSC in winter in the North Pacific activates anticyclone eddies in the central part of the deep BS in summer and fall (Fig. [A.10a](#)) and (with a 1-year lag) the anticyclone eddies located in the Aleutian North Slope Current area (Fig. [A.10c](#)). Our results support the conclusion of [Ladd et al. \(2012\)](#) who indicated that the anticyclonic eddy activity along the eastern shelf-break of the BS (the Pribilof eddy) during the spring months is negatively correlated with the North Pacific Index, a measure of the strength of the Aleutian Low in November–March. [Ladd et al. \(2012\)](#) assumed that a spin-up of the subpolar gyre in the northern North Pacific leads to increased eddy activity in the BS, possibly due to a local effect of the stronger Bering Slope Current or due to increased flow through the Aleutian passes.

Biological production in the deep basin of the BS is iron limited while the surface waters at the shelf are iron replete and nitrate limited ([Aguilar-Islas et al., 2007](#)). High surface chlorophyll *a* concentrations along the shelf break in the BS appears to be associated with an eddy-induced mixing between shelf and deep basin waters (see, e.g., [Okkonen et al., 2004](#); [Mizobata et al., 2008](#); [Ladd et al., 2012](#)). The mixing, induced by anticyclonic eddies between the low salinity coastal water and high salinity deep basin water, probably creates favourable conditions with a nitrate availability and a shallow pycnocline for the phytoplankton growth significantly increasing concentrations of chlorophyll *a* in the upper surface layer in the eastern BS in summer (Figs. [A.10a](#), [b](#) and [d](#)). The canyons, located at the shelf break (the Bering, Pribilof, Zhemchuk

and Navarin ones), are considered to be preferred sites of cross-shelf exchange (Clement Kinney et al., 2009).

An increase of the WSC in the northern North Pacific in winter impacts the mesoscale dynamics in the eastern subarctic Pacific and the eastern BS (Figs. 4 and A.10) and, thereby, a chlorophyll *a* concentration in surface waters (Fig. 6). Enhanced phytoplankton productivity in anticyclonic eddies may transfer up the food chain and results in increased biomass of higher trophic levels (zooplankton and fish). Advection paths of eggs and larvae can influence fish growth, survival and recruitment, either propelling them towards areas that support high growth and survival, or diverting them away from suitable habitat. For many fish species that spawn along the east subarctic continental slope, eggs and larvae benefit from slope to continental-shelf transport, where larvae encounter favorable feeding and growth conditions prior to the onset of winter (Bailey et al., 2008; Atwood et al., 2010). General biological efficiency, defined by success of reproduction of organisms at the lowest trophic levels, has priority value for formation of steady salmon feeding conditions.

In the western part of the BS the highest biomass of chum salmon has been observed at periphery of anticyclonic eddies where zooplankton is accumulated in the upper 100-meter layer (Sobolevsky et al., 1994). Moss et al. (2013) demonstrated that salmon, caught along the anticyclonic eddy's periphery in the eastern subarctic Pacific (the Sitka eddy), displayed the highest levels of insulin-like growth factor which is an index of the short-term growth rate for salmon. Zooplankton and phytoplankton densities are also greatest at the eddy's periphery. The location, timing and strength of the Sitka anticyclonic eddy, combined with juvenile salmon outmigration timing, could positively affect the growth by increased foraging opportunities. Years with enhanced production at the eddy's periphery and reduced inter- and intra-specific competition, resulting in increased survival for certain stocks (Moss et al., 2013), are those when the three primary eddy features in the eastern subarctic Pacific (the Haida, Sitka and Yakutat eddies) have been located close to the shore during early summer months when juvenile salmon are migrating to the north. The observed correlations between the WSC and salmon catches for the eastern subarctic Pacific and the eastern BS area (Figs. 7b–d) may be explained by an intensification (slow down) of the mesoscale dynamics and cross shelf exchange by macro- and micro- nutrients, stimulating phytoplankton and zooplankton growth forced by increased (decreased) WSC in the northern North Pacific in winter.

5. Conclusions

In this paper we proposed the forcing pattern that contributes to the interannual variability of the mesoscale dynamics and the chlorophyll *a* concentration in the surface waters in the Alaskan Stream area and the eastern Bering Sea. We conclude that the strength of the anticyclonic eddies along the deep basin slopes of the northern subarctic Pacific and the eastern Bering Sea is determined by the wind stress curl in the northern North Pacific in November–March. Strong correlations have been found between the concentrations of chlorophyll *a* at the shelf–deep-sea boundaries of the Bering Sea and the northern Pacific subarctic in August–September and the wind stress curl in the northern North Pacific in November–March. Our results indicate that the mesoscale dynamics in the eastern subarctic Pacific and the eastern Bering Sea areas may determine not only lower-trophic-level organism (autotrophic phytoplankton) biomass but also salmon abundance and catch.

Acknowledgements

The work was supported by the Russian Science Foundation (project no. 16–17–10025) and its methodological part was supported by the FEBRAS Program (No. AAAA-A17-117030110034-7). The altimeter products were distributed by AVISO with support from CNES.

Appendix A. Supplementary materials

Appendix A.1. Origin Lagrangian maps in the study area

We are interested in three different water masses and their transport pathways. To track the Alaskan Stream (AS) waters, the section along the meridian $x_0 = 145^\circ \text{ W}$ from $y_0 = 58^\circ \text{ N}$ to $y_0 = 60^\circ \text{ N}$ is fixed. The particles, which crossed that section in the past, are colored in red on the origin Lagrangian maps. The open-ocean particles, which crossed the section $x_0 = 160.0^\circ \text{ E} - 164.0^\circ \text{ W}$, $y_0 = 50.0^\circ \text{ N}$ in the past, are colored in green. The eastern Bering Sea (BS) particles, which crossed the section from 177.0° E , 62.0° N to 164° W , 55.0° N in the past, are colored in blue (see the yellow line in Fig. 2a). We removed from consideration all the particles entered into any AVISO grid cell with two or more corners touching the land in order to avoid artifacts due to the inaccuracy of the altimetry-based velocity field near the coast. The corresponding colored Lagrangian maps in Fig. A.8 demonstrate clearly origin, history and fate of those water masses in the study area.

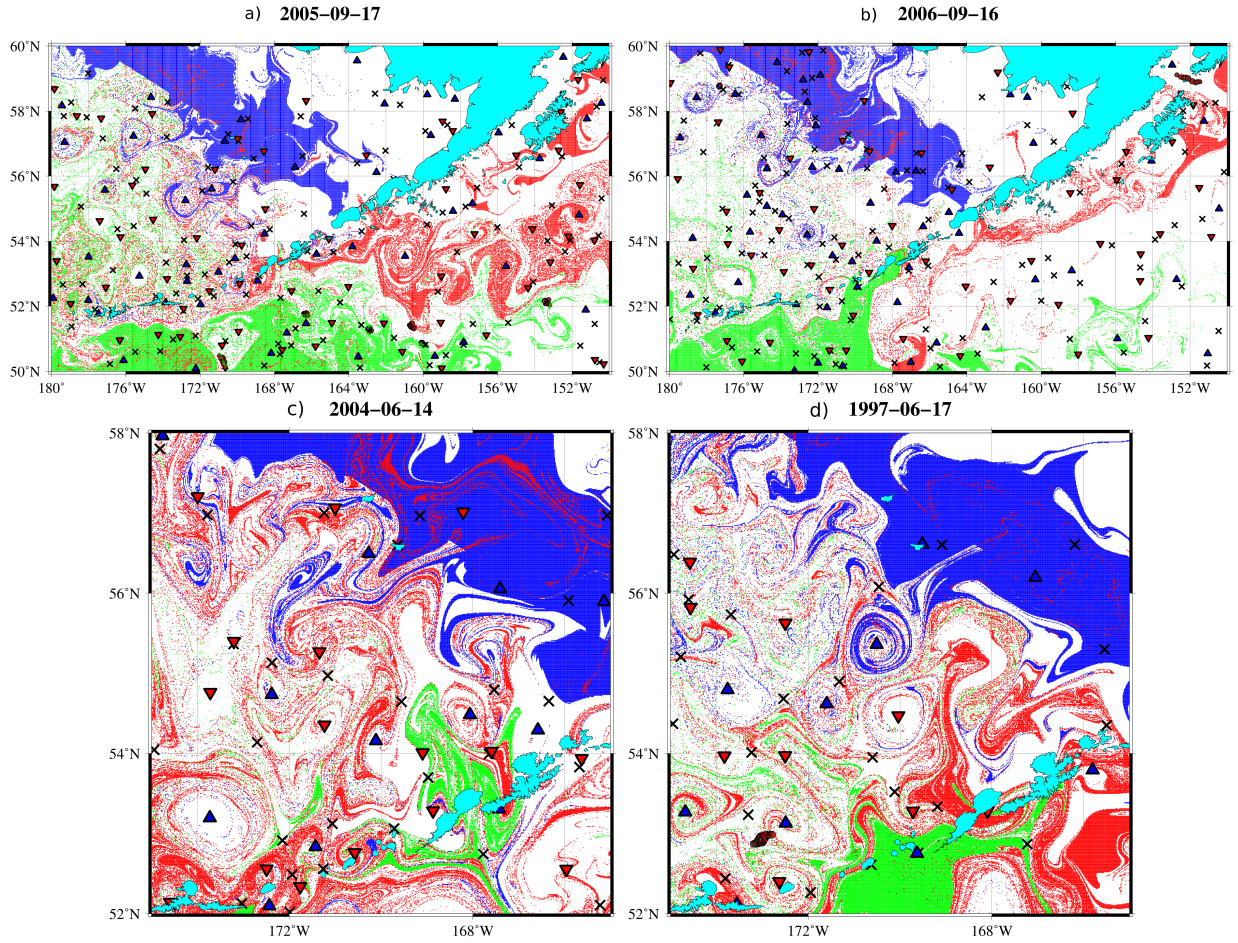


Figure A.8: The Lagrangian maps show transport pathways, origin, history and fate of Alaskan Stream (AS) (red), open-ocean (green) and Bering Sea (BS) (blue) waters in a) September 2005, b) September 2006, c) June 2004 (the center of the Pribiloff mesoscale anticyclone is at the point 54.5° N , 168° W) and d) June 1997 (the center of the Pribiloff mesoscale anticyclone is at the point 55.5° N , 171° W). The penetration of the BS shelf waters into the deep basin of the eastern BS is demonstrated by the blue color. Elliptic and hyperbolic stagnation points with zero velocity are indicated by triangles and crosses, respectively.

Appendix A.2. Vertical distributions of temperature, salinity and potential density inside and outside of the Alaskan Stream anticyclone in 2005–2006

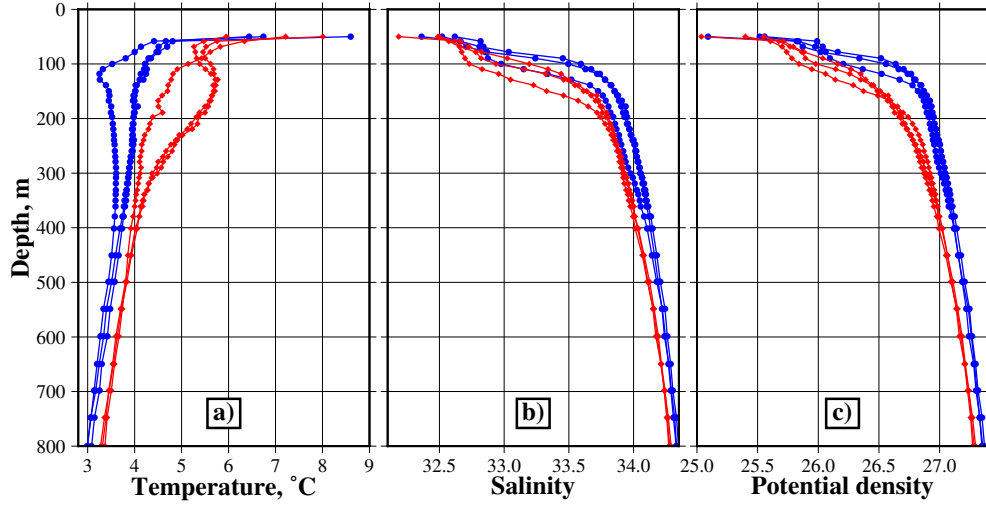


Figure A.9: The vertical distributions of temperature, salinity and relative density in September 2005 and 2006 inside (red color) and outside (blue color) the Alaskan Stream anticyclone 2005–2006 centered at around 54° N, 161° W in Fig. A.8a on 17 September 2005 and at 51° N, 167° W in Fig. A.8b on 16 September 2006. The data were taken from the Argo buoys nos. 4900342, 4900397, 4900646 and 4900705. Similar to ASAC 2003–2004 (see Figs. 2d–f), the ASAC 2005–2006 core was composed of relatively low salinity (33.7–33.9) and low density (26.7–26.9) waters. The temperature of waters inside of the anticyclone was 1–2 $^{\circ}$ C higher than outside it.

Appendix A.3. Annual changes of the wind stress curl in the northern North Pacific and the meridional and zonal velocities in the eastern Bering Sea

The changes in the Aleutian Low activity and the wind stress curl in the northern North Pacific in winter determine year-to-year changes in velocities in some areas of the eastern Bering Sea (see Fig. 4). An increase (decrease) of the WSC in the North Pacific in November–March is accompanied by increased (decreased) velocities at the boundaries of the anticyclonic eddies in the central part of the deep Bering Sea in summer and fall (Fig. A.10a). An intensification of the Aleutian Low and a large positive wind stress curl result in increasing of the northward flow on the Bering Sea outer shelf in the areas located close to the Pribiloff, Zhemchug and Navarin canyons (Fig. A.10b). An increase (decrease) of the wind stress curl in the northern North Pacific with a 1-year lag is accompanied by increased (decreased) velocities at the boundaries of the anticyclonic eddies located in the area of Aleutian North Slope Current in summer and fall (Fig. A.10c).

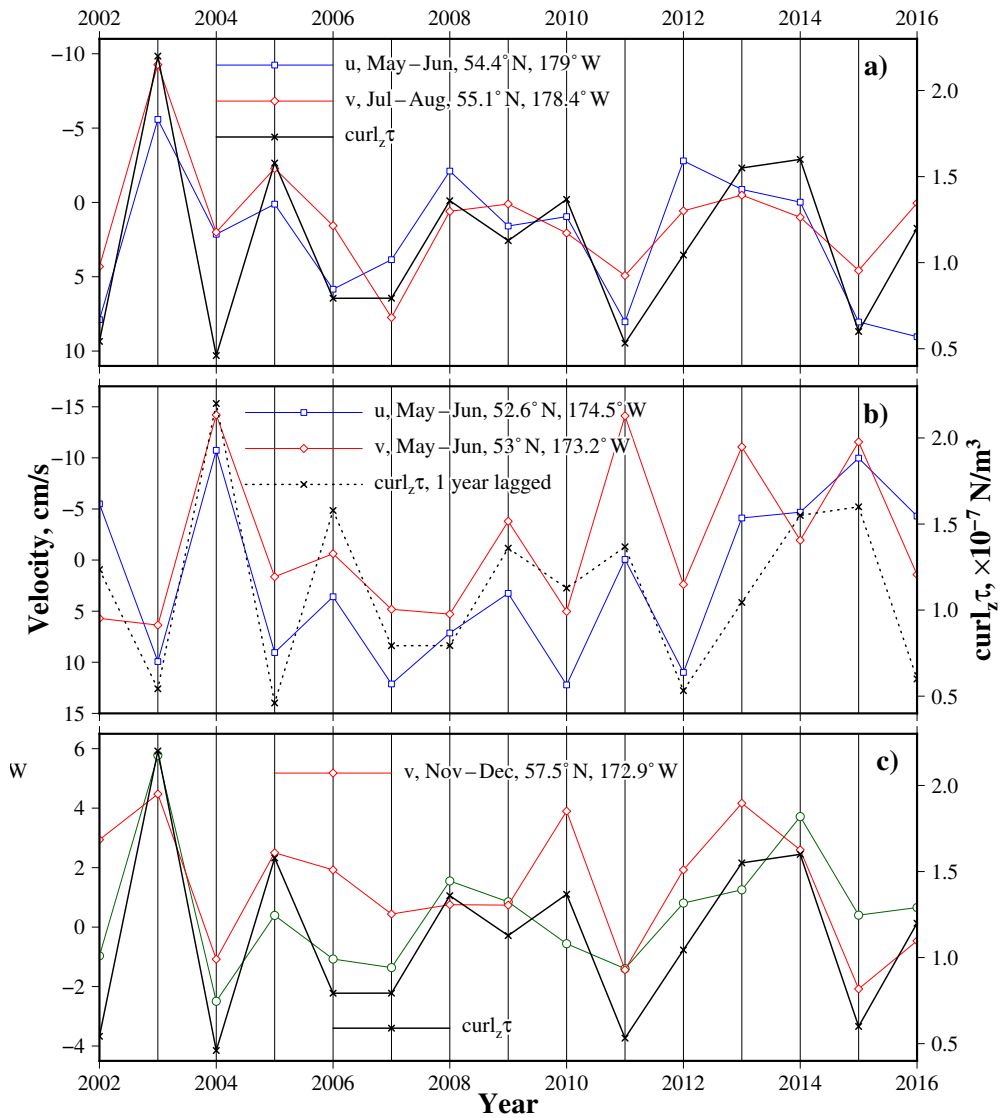


Figure A.10: a), b) and c) The year-to-year changes of the wind stress curl (November–March) in the northern North Pacific and the meridional and zonal velocities in the eastern Bering Sea.

Appendix A.4. Distribution of chlorophyll *a* concentration and salinity in the eastern Bering Sea

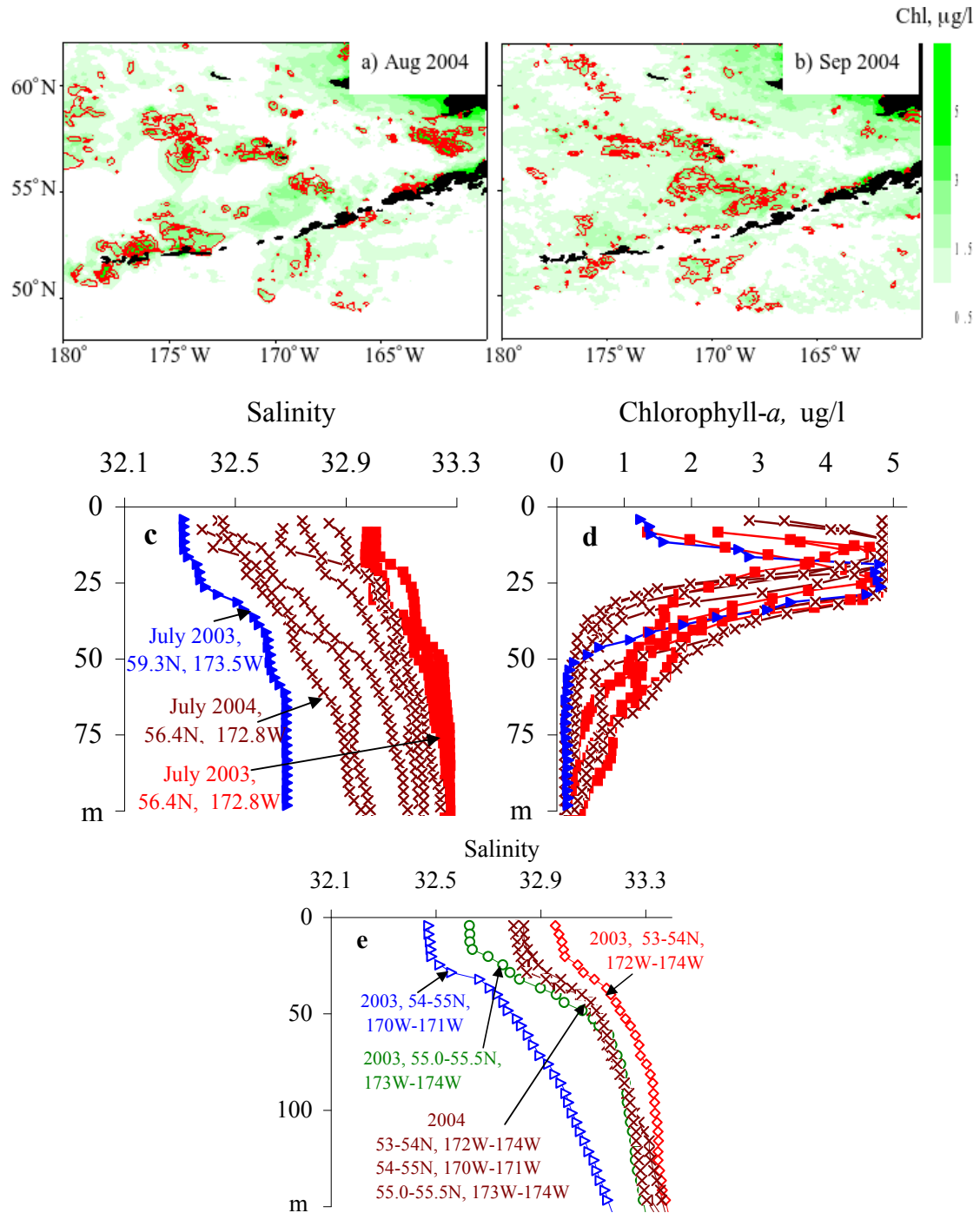


Figure A.11: a) and b) Distribution of the chlorophyll *a* concentration in August and September 2004 shown by the green color and the difference in chlorophyll *a* concentration between 2004 and 2003 shown by the red color lines; 1–5 $\mu\text{g/l}$ with the interval equal to 1 $\mu\text{g/l}$. c) and d) The vertical distributions of salinity and chlorophyll *a* in July 2003 and July 2004 in the eastern BS and e) the vertical distribution of salinity in the eastern Bering Sea in July–September 2003 and 2004 (the data from the Argo buoys nos. 4900142, 4900145, 4900165, 4900167 and 4900168).

Appendix A.5. The impact of anticyclonic eddies on the chlorophyll a distribution in the study area

The impact of anticyclonic eddies on the chlorophyll a distribution (the MODIS data) in the AS area can be demonstrated by using a Lagrangian indicator $L = \int_0^T \sqrt{u^2 + v^2} dt$ which is a measure of a distance passed by advected particles. A studied area has been seeded with a large number of virtual particles whose trajectories have been computed backward in time in the AVISO velocity field for a month from the date indicated on the corresponding maps. The L maps visualize not only the very vortex structures but also a history of water masses to be involved in the vortex motion in the past.

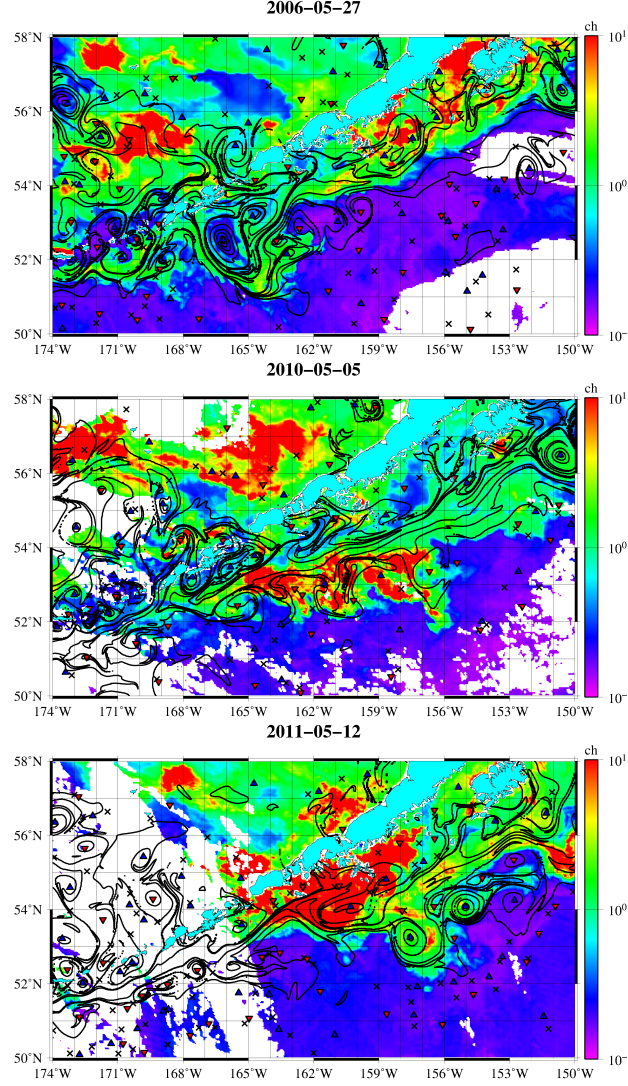


Figure A.12: The black isolines of the Lagrangian indicator L with the step of 200 geographic minutes imposed on the chlorophyll a distribution in the AS area (May 2006, May 2010 and May 2011). They enclose stable mesoscale eddies, such as ones with the elliptic points at 52.5° N, 165° W and at 53° N, 164° W. The dominant feature in the chlorophyll a distribution in the surface layer is a contrast between coastal and offshore waters. The coastal waters are productive with high values of chlorophyll a ($>6 \mu\text{g/l}$), and the off waters are oligotrophic with low chlorophyll a values ($<1 \mu\text{g/l}$). The filaments with high chlorophyll a concentration are wrapped around persistent mesoscale eddies.

References

- Aguilar-Islas, A.M., Hurst, M.P., Buck, K.N., Sohst, B., Smith, G.J., Lohan, M.C., Bruland, K.W., 2007. Micro- and macronutrients in the southeastern Bering Sea: Insight into iron-replete and iron-depleted regimes. *Progress in Oceanography* 73, 99–126. doi:[10.1016/j.pocean.2006.12.002](https://doi.org/10.1016/j.pocean.2006.12.002).
- Andreev, A.G., Baturina, V.I., 2006. Impacts of tides and atmospheric forcing variability on dissolved oxygen in the subarctic North Pacific. *Journal of Geophysical Research: Oceans* 111, C07S10. doi:[10.1029/2005jc003103](https://doi.org/10.1029/2005jc003103).
- Atwood, E., Duffy-Anderson, J.T., Horne, J.K., Ladd, C., 2010. Influence of mesoscale eddies on ichthyoplankton assemblages in the Gulf of Alaska. *Fisheries Oceanography* 19, 493–507. doi:[10.1111/j.1365-2419.2010.00559.x](https://doi.org/10.1111/j.1365-2419.2010.00559.x).
- Bailey, K.M., Abookire, A.A., Duffy-Anderson, J.T., 2008. Ocean transport paths for the early life history stages of offshore-spawning flatfishes: a case study in the Gulf of Alaska. *Fish and Fisheries* 9, 44–66. doi:[10.1111/j.1467-2979.2007.00268.x](https://doi.org/10.1111/j.1467-2979.2007.00268.x).
- Bond, N.A., Overland, J.E., Turet, P., 1994. Spatial and temporal characteristics of the wind forcing of the Bering Sea. *Journal of Climate* 7, 1119–1130. doi:[10.1175/1520-0442\(1994\)007<1139:satcot>2.0.co;2](https://doi.org/10.1175/1520-0442(1994)007<1139:satcot>2.0.co;2).
- Brown, J., Fiechter, J., 2012. Quantifying eddy–chlorophyll covariability in the Coastal Gulf of Alaska. *Dynamics of Atmospheres and Oceans* 55–56, 1–21. doi:[10.1016/j.dynatmoce.2012.04.001](https://doi.org/10.1016/j.dynatmoce.2012.04.001).
- Budyansky, M.V., Goryachev, V.A., Kaplunenko, D.D., Lobanov, V.B., Prants, S.V., Sergeev, A.F., Shlyk, N.V., Uleysky, M.Y., 2015. Role of mesoscale eddies in transport of Fukushima-derived cesium isotopes in the ocean. *Deep Sea Research Part I: Oceanographic Research Papers* 96, 15–27. doi:[10.1016/j.dsr.2014.09.007](https://doi.org/10.1016/j.dsr.2014.09.007).
- Clement Kinney, J., Maslowski, W., Okkonen, S., 2009. On the processes controlling shelf–basin exchange and outer shelf dynamics in the Bering Sea. *Deep Sea Research Part II: Topical Studies in Oceanography* 56, 1351–1362. doi:[10.1016/j.dsr2.2008.10.023](https://doi.org/10.1016/j.dsr2.2008.10.023).
- Combes, V., Di Lorenzo, E., 2007. Intrinsic and forced interannual variability of the Gulf of Alaska mesoscale circulation. *Progress in Oceanography* 75, 266–286. doi:[10.1016/j.pocean.2007.08.011](https://doi.org/10.1016/j.pocean.2007.08.011).
- Combes, V., Di Lorenzo, E., Curchitser, E., 2009. Interannual and decadal variations in cross-shelf transport in the Gulf of Alaska. *Journal of Physical Oceanography* 39, 1050–1059. doi:[10.1175/2008jpo4014.1](https://doi.org/10.1175/2008jpo4014.1).
- Crawford, W.R., Brickley, P.J., Peterson, T.D., Thomas, A.C., 2005. Impact of Haida Eddies on chlorophyll distribution in the Eastern Gulf of Alaska. *Deep Sea Research Part II: Topical Studies in Oceanography* 52, 975–989. doi:[10.1016/j.dsr2.2005.02.011](https://doi.org/10.1016/j.dsr2.2005.02.011).
- Crawford, W.R., Brickley, P.J., Thomas, A.C., 2007. Mesoscale eddies dominate surface phytoplankton in northern Gulf of Alaska. *Progress in Oceanography* 75, 287–303. doi:[10.1016/j.pocean.2007.08.016](https://doi.org/10.1016/j.pocean.2007.08.016).
- Cummins, P.F., Mysak, L.A., 1988. A quasi-geostrophic circulation model of the Northeast Pacific. Part I: A preliminary numerical experiment. *Journal of Physical Oceanography* 18, 1261–1286. doi:[10.1175/1520-0485\(1988\)018<1261:aqcmo>2.0.co;2](https://doi.org/10.1175/1520-0485(1988)018<1261:aqcmo>2.0.co;2).
- Favorite, F., 1974. *Oceanography of the Bering Sea with Emphasis on Renewable Resources*. Institute of Marine Science, University of Alaska. Chapter Flow into the Bering Sea through Aleutian Island passes. pp. 3–37.
- Henson, S.A., Thomas, A.C., 2008. A census of oceanic anticyclonic eddies in the Gulf of Alaska. *Deep Sea Research Part I: Oceanographic Research Papers* 55, 163–176. doi:[10.1016/j.dsr.2007.11.005](https://doi.org/10.1016/j.dsr.2007.11.005).
- Ishi, Y., 2005. Large-scale variabilities of wintertime wind stress curl field in the North Pacific and their relation to atmospheric teleconnection patterns. *Geophysical Research Letters* 32, L10607. doi:[10.1029/2004GL022330](https://doi.org/10.1029/2004GL022330).
- Johnson, G.C., Staben, P.J., Riser, S.C., 2004. The Bering slope current system revisited. *Journal of Physical Oceanography* 34, 384–398. doi:[10.1175/1520-0485\(2004\)034<0384:tbscsr>2.0.co;2](https://doi.org/10.1175/1520-0485(2004)034<0384:tbscsr>2.0.co;2).
- Johnson, K.W., Miller, L.A., Sutherland, N.E., Wong, C., 2005. Iron transport by mesoscale Haida eddies in the Gulf of Alaska. *Deep Sea Research Part II: Topical Studies in Oceanography* 52, 933–953. doi:[10.1016/j.dsr2.2004.08.017](https://doi.org/10.1016/j.dsr2.2004.08.017).
- Ladd, C., Mordy, C.W., Kachel, N.B., Staben, P.J., 2007. Northern Gulf of Alaska eddies and associated anomalies. *Deep Sea Research Part I: Oceanographic Research Papers* 54, 487–509. doi:[10.1016/j.dsr.2007.01.006](https://doi.org/10.1016/j.dsr.2007.01.006).
- Ladd, C., Staben, P., Cokelet, E., 2005. A note on cross-shelf exchange in the northern Gulf of Alaska. *Deep Sea Research Part II: Topical Studies in Oceanography* 52, 667–679. doi:[10.1016/j.dsr2.2004.12.022](https://doi.org/10.1016/j.dsr2.2004.12.022).
- Ladd, C., Staben, P.J., O'Hern, J.E., 2012. Observations of a Pribilof eddy. *Deep Sea Research Part I: Oceanographic Research Papers* 66, 67–76. doi:[10.1016/j.dsr.2012.04.003](https://doi.org/10.1016/j.dsr.2012.04.003).
- Melsom, A., Metzger, E.J., Hurlburt, H.E., 2003. Impact of remote oceanic forcing on Gulf of Alaska sea levels and mesoscale circulation. *Journal of Geophysical Research: Oceans* 108, 3346. doi:[10.1029/2002jc001742](https://doi.org/10.1029/2002jc001742).
- Mizobata, K., Saitoh, S.I., Shiomoto, A., Miyamura, T., Shiga, N., Imai, K., Toratani, M., Kajiwara, Y., Sasaoka, K., 2002. Bering Sea cyclonic and anticyclonic eddies observed during summer 2000 and 2001. *Progress in Oceanography* 55, 65–75. doi:[10.1016/S0079-6611\(02\)00070-8](https://doi.org/10.1016/S0079-6611(02)00070-8).
- Mizobata, K., Saitoh, S.I., Wang, J., 2008. Interannual variability of summer biochemical enhancement in relation to mesoscale eddies at the shelf break in the vicinity of the Pribilof Islands, Bering Sea. *Deep Sea Research Part II: Topical Studies in Oceanography* 55, 1717–1728. doi:[10.1016/j.dsr2.2008.03.002](https://doi.org/10.1016/j.dsr2.2008.03.002).
- Mizobata, K., Wang, J., Saitoh, S.I., 2006. Eddy-induced cross-slope exchange maintaining summer high productivity of the Bering Sea shelf break. *Journal of Geophysical Research: Oceans* 111, C10017. doi:[10.1029/2005JC003335](https://doi.org/10.1029/2005JC003335).
- Mordy, C.W., Staben, P.J., Ladd, C., Zeeman, S., Wisegarver, D.P., Salo, S.A., Hunt, G.L., 2005. Nutrients and primary production along the eastern Aleutian Island Archipelago. *Fisheries Oceanography* 14, 55–76. doi:[10.1111/j.1365-2419.2005.00364.x](https://doi.org/10.1111/j.1365-2419.2005.00364.x).
- Moss, J., Trudel, M., Beckman, B., Crawford, W., Fournier, W., Fergusson, E., Beacham, T., 2013. Benefits of living life on the edge: Enhanced growth and foraging opportunities for juvenile salmon inhabiting the margins of the Sitka Eddy.

- North Pacific Anadromous Fish Commission Technical Report 9, 77–78. URL: <http://www.npafc.org/new/publications/Technical%20Report/TR9/Moss%20et%20al.pdf>.
- Myers, K.W., Klovach, N.V., Gritsenko, O.F., Urawa, S., Royer, T.C., 2007. Stock-specific distributions of Asian and North American salmon in the open ocean, interannual changes, and oceanographic conditions. *North Pacific Anadromous Fish Commission Bulletin* 4, 159–177. URL: <http://www.npafc.org/new/publications/Bulletin/Bulletin%20No.%204/159-177Myers.pdf>.
- Okkonen, S.R., Jacobs, G.A., Joseph Metzger, E., Hurlburt, H.E., Shriver, J.F., 2001. Mesoscale variability in the boundary currents of the Alaska Gyre. *Continental Shelf Research* 21, 1219–1236. doi:10.1016/S0278-4343(00)00085-6.
- Okkonen, S.R., Schmidt, G., Cokelet, E., Stabeno, P., 2004. Satellite and hydrographic observations of the Bering Sea ‘Green Belt’. *Deep Sea Research Part II: Topical Studies in Oceanography* 51, 1033–1051. doi:10.1016/S0967-0645(04)00099-2.
- Okkonen, S.R., Weingartner, T.J., Danielson, S.L., Musgrave, D.L., Schmidt, G.M., 2003. Satellite and hydrographic observations of eddy-induced shelf-slope exchange in the northwestern Gulf of Alaska. *Journal of Geophysical Research: Oceans* 108, 3033. doi:10.1029/2002jc001342.
- Prants, S.V., Andreev, A.G., Budyansky, M.V., Uleysky, M.Y., 2013a. Impact of mesoscale eddies on surface flow between the Pacific Ocean and the Bering Sea across the Near Strait. *Ocean Modelling* 72, 143–152. doi:10.1016/j.ocemod.2013.09.003.
- Prants, S.V., Andreev, A.G., Budyansky, M.V., Uleysky, M.Y., 2015. Impact of the Alaskan Stream flow on surface water dynamics, temperature, ice extent, plankton biomass, and walleye pollock stocks in the eastern Okhotsk Sea. *Journal of Marine Systems* 151, 47–56. doi:10.1016/j.jmarsys.2015.07.001.
- Prants, S.V., Budyansky, M.V., Uleysky, M.Y., 2014. Identifying Lagrangian fronts with favourable fishery conditions. *Deep Sea Research Part I: Oceanographic Research Papers* 90, 27–35. doi:10.1016/j.dsr.2014.04.012.
- Prants, S.V., Lobanov, V.B., Budyansky, M.V., Uleysky, M.Y., 2016. Lagrangian analysis of formation, structure, evolution and splitting of anticyclonic Kuril eddies. *Deep Sea Research Part I: Oceanographic Research Papers* 109, 61–75. doi:10.1016/j.dsr.2016.01.003.
- Prants, S.V., Ponomarev, V.I., Budyansky, M.V., Uleysky, M.Y., Fayman, P.A., 2013b. Lagrangian analysis of mixing and transport of water masses in the marine bays. *Izvestiya, Atmospheric and Oceanic Physics* 49, 82–96. doi:10.1134/S0001433813010088.
- Prants, S.V., Uleysky, M.Y., Budyansky, M.V., 2017. *Lagrangian Oceanography: Large-scale Transport and Mixing in the Ocean*. Physics of Earth and Space Environments, Springer. doi:10.1007/978-3-319-53022-2.
- Qiu, B., 2002. Large-scale variability in the midlatitude subtropical and subpolar North Pacific Ocean: Observations and causes. *Journal of Physical Oceanography* 32, 353–375. doi:10.1175/1520-0485(2002)032<0353:LSVITM>2.0.CO;2.
- Sato, S., Moriya, S., Azumaya, T., Nagoya, H., Abe, S., Urawa, S., 2009. Stock distribution patterns of chum salmon in the Bering Sea and north Pacific Ocean during the summer and fall of 2002–2004. *North Pacific Anadromous Fish Commission Bulletin* 5, 29–37. URL: [http://www.npafc.org/new/publications/Bulletin/Bulletin%20No.%205/NPAFC_Bull_5_029-037\(Sato\).pdf](http://www.npafc.org/new/publications/Bulletin/Bulletin%20No.%205/NPAFC_Bull_5_029-037(Sato).pdf).
- Schumacher, J.D., Stabeno, P.J., Roach, A.T., 1989. Volume transport in the Alaska Coastal Current. *Continental Shelf Research* 9, 1071–1083. doi:10.1016/0278-4343(89)90059-9.
- Sobolevsky, E., Radchenko, V., Startsev, A., 1994. Distribution and feeding of chum salmon in the western part of the Bering Sea and pacific waters off Kamchatka. *Voprosy Ihtiologii* 34, 35–40. [in Russian].
- Springer, A.M., McRoy, C.P., Flint, M.V., 1996. The Bering Sea Green Belt: shelf-edge processes and ecosystem production. *Fisheries Oceanography* 5, 205–223. doi:10.1111/j.1365-2419.1996.tb00118.x.
- Stabeno, P.J., Kachel, D.G., Kachel, N.B., Sullivan, M.E., 2005. Observations from moorings in the Aleutian Passes: temperature, salinity and transport. *Fisheries Oceanography* 14, 39–54. doi:10.1111/j.1365-2419.2005.00362.x.
- Stabeno, P.J., Ladd, C., Reed, R.K., 2009. Observations of the Aleutian North Slope Current, Bering Sea, 1996–2001. *Journal of Geophysical Research: Oceans* 114, C05015. doi:10.1029/2007jc004705.
- Stabeno, P.J., Reed, R.K., 1994. Circulation in the Bering Sea basin observed by satellite-tracked drifters: 1986–1993. *Journal of Physical Oceanography* 24, 848–854. doi:10.1175/1520-0485(1994)024<0848:CITBSB>2.0.CO;2.
- Ueno, H., Crawford, W.R., Onishi, H., 2010. Impact of Alaskan Stream eddies on chlorophyll distribution in the North Pacific. *Journal of Oceanography* 66, 319–328. doi:10.1007/s10872-010-0028-6.